

## ***Ab initio* Structure Determination of [(Dimethylamino)methylene]bis[phosphonic Acid] Dihydrate from X-Ray Powder Diffraction Data: Comparison with the Corresponding Monohydrate and Unhydrated Form**

by **Antonia Neels\*** and **Helen Stoeckli-Evans**

Institut de Chimie, Université de Neuchâtel, Avenue de Bellevaux 51, CH-2000 Neuchâtel

and **Burkhard Costisella**

Fachbereich Chemie, Universität Dortmund, D-44221 Dortmund

and **Harald Jancke**

Bundesanstalt für Materialforschung und -prüfung, Rudower Chaussee 5, D-12489 Berlin

and **Kenneth D. Knudsen** and **Philip Pattison**

Swiss-Norwegian Beam Line at ESRF, BP 220, F-38043 Grenoble Cédex

---

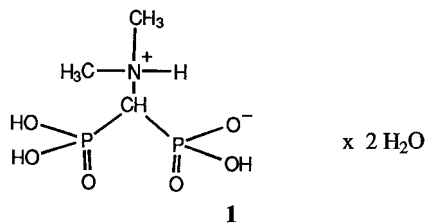
The structure of [(dimethylamino)methylene]bis[phosphonic acid] dihydrate ( $C_3H_{11}NO_6P_2 \cdot 2H_2O$ ; **1**) was solved *ab initio* from synchrotron powder X-ray diffraction data. The structure determination was based on direct methods combined with difference *Fourier* techniques, and the refinement was carried out using the *Rietveld* method. Using this high-quality diffraction pattern, it was possible to index a second phase which corresponds to the structure of the known [(dimethylamino)methylene]bis[phosphonic acid] monohydrate (**2**). [(Dimethylamino)methylene]bis[phosphonic acid] dihydrate (**1**) is monoclinic, space group  $P2_1/c$ ,  $Z = 4$ , with  $a = 10.6644(1)$ ,  $b = 9.1599(1)$ ,  $c = 10.5213(1)$  Å, and  $\beta = 98.353(1)^\circ$ . The structure analysis indicates two non-equivalent P-atoms in the molecule of **1** which are also observed in the corresponding monohydrate **2** and unhydrated form **3**. All three compounds exhibit extended H-bonding networks which result in remarkably different  $^{31}P$ -NMR spectra. The [(dimethylamino)methylene]bis[phosphonic acids] **1–3** crystallize in the betaine-type structure which, therefore, contains two nonequivalent P-atoms. The  $-P(=O)(OH)_2$  and  $-P(=O)(OH)O^-$  groups of **1–3** are involved in a number of strong H-bonds which can be characterized by the different  $^{31}P$ -NMR chemical shifts of the two P-atoms of **1–3**.

---

**1. Introduction.** – Phosphonic acids are of interest from the standpoint of their chelating properties [1][2] and from their use in modern *in vivo* diagnostic techniques [3]. Additional interest stems from their resemblance to amino acids and from the fact that some aminophosphonic-acid derivatives have been found in lower animals and that these compounds seem to play a role in the metabolism of these organisms [4].

[(Dimethylamino)methylene]bis[phosphonic acid] ( $C_3H_{11}NO_6P_2$ ) is an organophosphorous compound containing P–C bonds. It has been prepared and structurally characterized in its unhydrated form, *i.e.*,  $C_3H_{11}NO_6P_2$  (**3**) [5][6]. The molecular structure of the monohydrated compound, *i.e.*,  $C_3H_{11}NO_6P_2 \cdot H_2O$  (**2**), has also been reported [7]. The formation of a dihydrated form of the same compound, *i.e.*,  $C_3H_{11}NO_6P_2 \cdot 2H_2O$  (**1**) was discussed [8], but no crystal structure has been reported until now. While macroscopic-sized single crystals of the unhydrated form **3** and of the

monohydrate **2** could be easily obtained for single-crystal structure analysis, the [(dimethylamino)methylene]bis[phosphonic acid] dihydrate (**1**) was obtained only in microcrystalline form. Using powder diffraction techniques, we have now succeeded in solving the molecular structure of **1**.



$^{31}\text{P}$ -NMR Studies in liquid and solid state have been reported for all three samples **1–3** by *Harris et al.* [9] and *Jancke et al.* [8]. The knowledge of the structures presents a rare possibility of direct elucidation of the influence of water and the formation of H-bonds on the configuration of such a molecule. We now report on the relationship between the crystal structures and the properties, such as solid-state  $^{31}\text{P}$ -NMR data, of dihydrate **1**, of monohydrate **2**, and of the unhydrated form **3**.

**2. Experimental** – [(Dimethylamino)methylene]bis[phosphonic acid] dihydrate ( $\text{C}_3\text{H}_{11}\text{NO}_6\text{P}_2 \cdot 2\text{H}_2\text{O}$ , **1**) was obtained in microcrystalline form by precipitation from an aq. soln. by means of acetone. Slow recrystallization from  $\text{H}_2\text{O}$  yielded crystals of the unhydrated form **3** [8].

For compound **1**, the X-ray powder diffraction data were first collected on a finely ground sample (side-loaded in a flat sample holder) using a *Rigaku* computer automated diffractometer. The X-ray source was a rotating anode operating at 50 kV and 180 mA with a copper target and graphite monochromated radiation. Data were collected between 5 and 80° in  $2\theta$  with a step size of 0.01° and a counting time of 10 s/step (*Fig. 1.a*). The indexing procedure [10] revealed a monoclinic cell with  $a = 10.66$ ,  $b = 9.16$ ,  $c = 10.53$  Å, and  $\beta = 98.34^\circ$ . The presence of a second phase in the sample was suggested by a relatively intensive reflection at 7.248° ( $2\theta$ ) which could not be indexed. The structure solution using the indexed monoclinic unit cell and the derived space group  $P2_1/c$  by direct methods and *Patterson* search failed. The compound was then remeasured in transmission mode using synchrotron radiation at the Swiss-Norwegian beamline, ESRF (*Fig. 1.b*). From the high-resolution synchrotron X-ray powder data, ca. 700 reflections were extracted using the program EXPO [11]. The main structure of **1** was solved by direct methods using SHELXS [12] and completed by difference *Fourier* techniques [13].

The obtained structural model was used for *Rietveld* profile refinement in GSAS [14] using the profile over the range  $3^\circ < 2\theta < 45^\circ$ . After the initial refinement of the scale, background, and unit-cell constants, the non-H-atom positions were refined without constraining the bond lengths and angles. The H-atoms of the Me and CH groups, and the H-atom attached to the N-atom of the dimethylamino group were introduced in their calculated positions in analogy to the procedure used in the case of the monohydrate **2** and the unhydrated form **3**. The remaining H-atoms of the phosphonic-acid moieties and the H-atoms of the  $\text{H}_2\text{O}$  molecules were placed in positions of significant positive electron density located in *Fourier* difference syntheses. The introduction of the H-atoms gave slightly lower *R* values than without H-atoms:  $wR2$  0.112 vs. 0.118 (without H-atoms), *R*1 0.080 vs. 0.084, and *R<sub>f</sub>* 0.062 vs. 0.066. The refinement for the H-atoms was constrained using normal O–H bond lengths and P–O–H and H–O–H bond angles and an overall isotropic temperature factor. In the final cycles of refinement, the shifts in all parameters were less than their estimated standard deviations. The high quality of the diffraction pattern permitted the second phase to be indexed, and it was found to arise from the structure of the known [(dimethylamino)methylene]bis[phosphonic acid] monohydrate (**2**) [7].

Crystallographic details for **1** are given in *Table 1*, and *Fig. 2* illustrates the final *Rietveld* plot showing the simultaneous refinement of two phases (95% of **1** and 5% of **2**). Selected bond lengths and angles and a list of important intermolecular  $\text{N} \cdots \text{O}$  and  $\text{O} \cdots \text{O}$  distances of **1–3** are given in *Tables 2* and *3*, resp. For monohydrate **2**, the atom positions in the corresponding unit cell were used with their original values [7] and kept constant

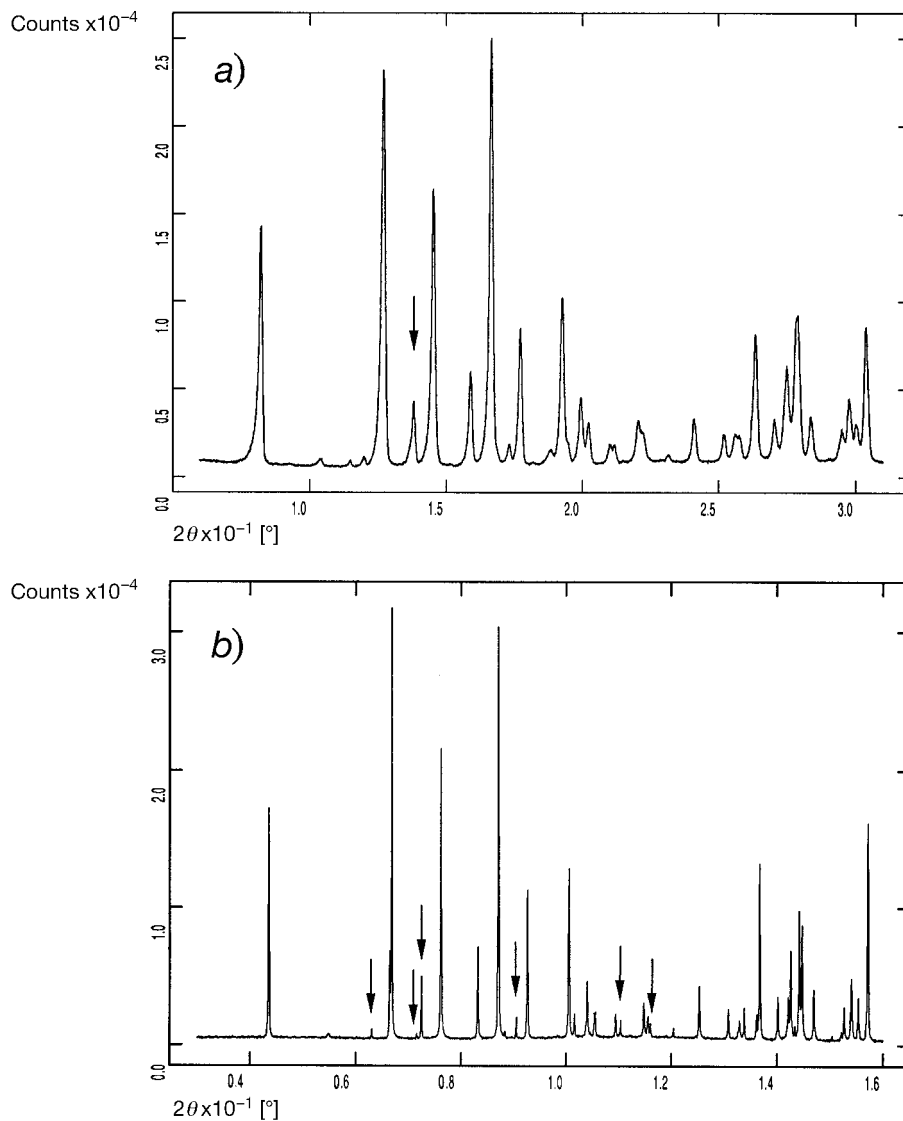


Fig. 1. Powder diffraction profile for dihydrate **1**: a) low-angle part of the data measured in reflection mode using copper ( $K\alpha_1 + K\alpha_2$ ) radiation, b) data measured in transmission mode using synchrotron radiation. Reflections of the second phase, i.e., of monohydrate **2** (5%), are marked by arrows.

during the *Rietveld* refinement procedure; only the profile parameters were refined for this second phase. Crystallographic data for the structures discussed in this paper have been deposited with the *Cambridge Crystallographic Data Centre* as deposition No. CCDC-102870 for **1** and CCDC-102871 for **2**. Copies of the data can be obtained, free of charge, on application to the CCDC, 12 Union Road, Cambridge CB2 1EZ, UK.

Table 1. Crystallographic Data for Dihydrate **1**

Formula	C <sub>3</sub> H <sub>11</sub> NO <sub>6</sub> P <sub>2</sub> ·2H <sub>2</sub> O	T [K]	296
Formula weight	255.13	$\rho_{\text{calc}}$ [g/cm <sup>-3</sup> ]	1.679
[g/mol]		$\mu$ [mm <sup>-1</sup> ]	0.45
Crystal system	monoclinic	Pattern range (2 $\theta$ )	3–45°
Space group	P2 <sub>1</sub> /c (No. 14)	Step size (2 $\theta$ )	0.005°
a [Å]	10.6644(1)	2 $\theta$ Interval [°]/step scan time [s]	3–18/4; 18–45/8
b [Å]	9.1599(1)	Data collection mode	transmission (1.0-mm capillary)
c [Å]	10.5213(1)	No. of contributing reflections	1450 (phase I and II)
$\beta$ [°]	98.353(1)	No. of structural parameters	105
V [Å <sup>3</sup> ]	1016.86(1)	No. of profile parameters	9
Z	4	$R_{\text{wp}}^{\text{a}}/R_p^{\text{b}}$	0.112/0.080
$\lambda$ [Å]	0.79934	$R_F^{\text{c}}$	0.065

<sup>a</sup>)  $R_{\text{wp}} = [\sum w(I_o - I_c)^2 / \sum wI_o^2]^{1/2}$ . <sup>b</sup>)  $R_p = \sum |I_o - I_c| / \sum I_c$ . <sup>c</sup>)  $R_F = (|F_o| - |F_c|) / |F_o|$ .

Table 2. Selected Bond Lengths [Å] and Bond Angles [°] for **1–3**. Arbitrary numbering.

	<b>1</b>	<b>2</b> [7]	<b>3</b> [6]		<b>1</b>	<b>2</b> [7]	<b>3</b> [6]
P(1)–O(1)	1.55(1)	1.504	1.494 <sup>a</sup> )	O(1)–P(1)–O(2)	120.5(6)	115.4	116.6
P(1)–O(2)	1.57(1) <sup>a</sup> )	1.461 <sup>a</sup> )	1.510	O(1)–P(1)–O(3)	108.8(6)	109.7	111.9
P(1)–O(3)	1.51(1)	1.550	1.555	O(1)–P(1)–C(1)	98.7(7)	103.1	105.7
P(1)–C(1)	1.88(1)	1.906	1.841	O(2)–P(1)–O(3)	108.5(7)	115.7	108.6
P(2)–O(4)	1.54(1)	1.577	1.481 <sup>a</sup> )	O(2)–P(1)–C(1)	110.6(7)	108.9	107.6
P(2)–O(5)	1.49(1) <sup>a</sup> )	1.505	1.515	O(3)–P(1)–C(1)	109.0(6)	102.5	105.8
P(2)–O(6)	1.59(1)	1.461 <sup>a</sup> )	1.555	O(4)–P(2)–O(5)	114.4(6)	110.9	117.8
P(2)–C(1)	1.78(1)	1.845	1.842	O(4)–P(2)–O(6)	105.8(6)	108.1	107.6
C(1)–N(1)	1.57(1)	1.510	1.516	O(4)–P(2)–C(1)	108.8(7)	103.5	108.7
N(1)–C(2)	1.49(1)	1.510	1.503	O(5)–P(2)–O(6)	113.4(6)	118.6	111.7
N(1)–C(3)	1.40(1)	1.497	1.497	O(5)–P(2)–C(1)	106.0(7)	103.4	102.7
				O(6)–P(2)–C(1)	107.6(7)	111.3	107.9
				C(1)–N(1)–C(2)	115.2(11)	114.4	116.2
				C(1)–N(1)–C(3)	116.8(12)	112.1	112.4
				C(2)–N(1)–C(3)	111.6(11)	110.6	110.1
				P(1)–C(1)–P(2)	118.1(8)	112.2	113.8
				P(1)–C(1)–N(1)	110.4(10)	116.1	115.6
				P(2)–C(1)–N(1)	112.5(10)	112.4	112.0

<sup>a</sup>) Formal P=O bonds.

**3. Results and Discussion.** – The structure analysis of dihydrate **1** indicates two non-equivalent P-atoms in the molecule, which was also observed in the case of the corresponding monohydrate **2** and unhydrated form **3**. The protonation of the N-atom is responsible for the formation of an intramolecular H-bond, and consequently for the formation of the different H-bonding situations due to the formation of one phosphonic-acid group (–P(=O)(OH)<sub>2</sub>) and one phosphonate-anion group (–P(=O)(OH)O<sup>-</sup>) (Fig. 3). The atoms P(1) and P(2) display tetrahedral environments with normal bond lengths and angles which are similar to those found for compounds **2** and **3** by single-crystal structure analyses (Table 2), within experimental error. However, the precision of the powder diffraction analysis is much lower than that of the single-crystal structure analyses. All the non-H-atoms in the powder structure **1**

Table 3.  $N\cdots O$  and  $O\cdots O$  Hydrogen Bond Distances [ $\text{\AA}$ ] for **1–3**. Arbitrary numbering.

<b>1</b>	<b>2</b>	<b>3</b>
Intramolecular interactions:		
N(1)–H $\cdots$ O(4) 2.97(1)	N(1)–H $\cdots$ O(4) 2.94	N(1)–H $\cdots$ O(4) 2.92
Intermolecular interactions:		
Environment of P(1):		
O(1)–H $\cdots$ O(2W) <sup>a</sup> 2.49(2)	O(1)–H $\cdots$ O(1W) <sup>g</sup> 2.46	O(6) <sup>n</sup> –H $\cdots$ O(1) 2.58
O(1W) <sup>b</sup> –H $\cdots$ O(2) 2.68(1)	O(1W) <sup>i</sup> –H $\cdots$ O(2) 2.78	O(2) $\cdots$ H $\cdots$ O(5) <sup>o</sup> 2.41
O(2W)–H $\cdots$ O(2) 2.57(1)	O(4) <sup>h</sup> –H $\cdots$ O(2) 2.64	O(3)–H $\cdots$ O(4) <sup>m</sup> 2.51
O(3)–H $\cdots$ O(5) <sup>c</sup> 2.57(1)	O(3)–H $\cdots$ O(5) <sup>l</sup> 2.42	N(1)–H $\cdots$ O(1) <sup>p</sup> 2.82
Environment of P(2):		
O(1W)–H $\cdots$ O(4) 2.73(1)	O(4)–H $\cdots$ O(2) <sup>k</sup> 2.64	O(3) <sup>p</sup> –H $\cdots$ O(4) 2.51
O(2W) <sup>d</sup> –H $\cdots$ O(4) 2.38(1)	O(3) <sup>j</sup> –H $\cdots$ O(5) 2.42	O(5) $\cdots$ H $\cdots$ O(2) <sup>q</sup> 2.41
O(3) <sup>e</sup> –H $\cdots$ O(5) 2.57(1)	O(1W)–H $\cdots$ O(6) 2.66	O(6)–H $\cdots$ O(1) <sup>n</sup> 2.58
O(6)–H $\cdots$ O(1W) <sup>e</sup> 2.56(1)	N(1)–H $\cdots$ O(6) <sup>k</sup> 2.87	
N(1)–H $\cdots$ O(5) <sup>f</sup> 2.79(1)		

<sup>a</sup>)  $x, 1/2 - y, 1/2 + z$ . <sup>b</sup>)  $-x, -1/2 + y, 1/2 - z$ . <sup>c</sup>)  $1 - x, 1 - y, 1 - z$ . <sup>d</sup>)  $x, 1 + y, z$ . <sup>e</sup>)  $x, 3/2 - y, 1/2 + z$ . <sup>f</sup>)  $x, 3/2 - y, -1/2 + z$ .  
<sup>g</sup>)  $x, 1 + y, z$ . <sup>h</sup>)  $1/2 - x, y, -1/2 + z$ . <sup>i</sup>)  $-1/2 + x, 1 - y, z$ . <sup>j</sup>)  $-1/2 + x, 2 - y, z$ . <sup>k</sup>)  $1/2 - x, y, 1/2 + z$ . <sup>l</sup>)  $1/2 + x, 2 - y, z$ .  
<sup>m</sup>)  $x, 1/2 + y, 1/2 - z$ . <sup>n</sup>)  $-x, 1 - y, -z$ . <sup>o</sup>)  $1 + x, y, z$ . <sup>p</sup>)  $-x, -1/2 + y, 1/2 - z$ . <sup>q</sup>)  $-1 + x, y, z$ .

were freely refined. This was possible using the high-resolution synchrotron powder diffraction data, but the lack of data (limited number of reflections, 2-phase system) results in small deviations from standard values and relatively high standard deviations for bond lengths and bond angles. The standard deviations given in *Table 2* for **1**, are certainly underestimated. This is demonstrated by the large range found for the C–N bond length values (1.40(1), 1.49(1), and 1.57(1)  $\text{\AA}$ ) as compared to the standard value of 1.50  $\text{\AA}$  [15]. This same bond length varies from 1.497 to 1.510  $\text{\AA}$  in **2** [4] and from 1.497 to 1.516  $\text{\AA}$  in **3** [5][6]. The P–C bond lengths are 1.88(1) and 1.78(1) in **1**, 1.906 and 1.845  $\text{\AA}$  in **2**, and 1.841 and 1.842  $\text{\AA}$  in **3**. The P–O(terminal) bond lengths vary from 1.49(1) to 1.59(1)  $\text{\AA}$  (P–O<sub>av</sub> 1.54  $\text{\AA}$ ). Formal double bonds are assigned to P–O(5) (1.49(1)  $\text{\AA}$ ) and P–O(2) (1.57(1)  $\text{\AA}$ ), even though the latter exhibits a relatively large deviation from the normal bond-length range of P=O bonds (1.45–1.50  $\text{\AA}$  [15]). This is probably due to the low precision of the powder structure analysis. All the P(1)–O bonds show bond lengths in the range of 1.51–1.57  $\text{\AA}$ . Atom O(5), being double-bonded to P(2), is involved in an intermolecular H-contact to atom O(3) (2.57(1)  $\text{\AA}$ ). Positive electron density is located near to O(3) and assigned to a H-atom, hence, atom O(3) is assumed to belong to an OH group. A practically eclipsed conformation of the phosphonic-acid and phosphonate-anion groups of **1** is observed, which is reflected in the torsion angles O–P $\cdots$ P–O along the P $\cdots$ P direction (the three smallest torsion angles are 21, 26, and 57°).

All six O-atoms O(1) to O(6) of **1** are involved in the H-bonding network (*Fig. 4*). An intramolecular H-bond is formed between the NH proton and atom O(4). The torsion angle N(1)–C(1)–P(2)–O(4) is 30.3° and comparable to the corresponding torsion angle in **2** (34.9°) and **3** (23.8°). Each water molecule of **1**, symbolized by the O-atoms O(W1) and O(W2), participates in three H-bond contacts, *i.e.*, in two donor bonds involving the water H-atoms (O(1W)<sup>b</sup>)–H $\cdots$ O(2) and O(1W)–H $\cdots$ O(4), and O(2W)–H $\cdots$ O(2) and O(2W)<sup>d</sup>)–H $\cdots$ O(4), resp.) and in one acceptor bond

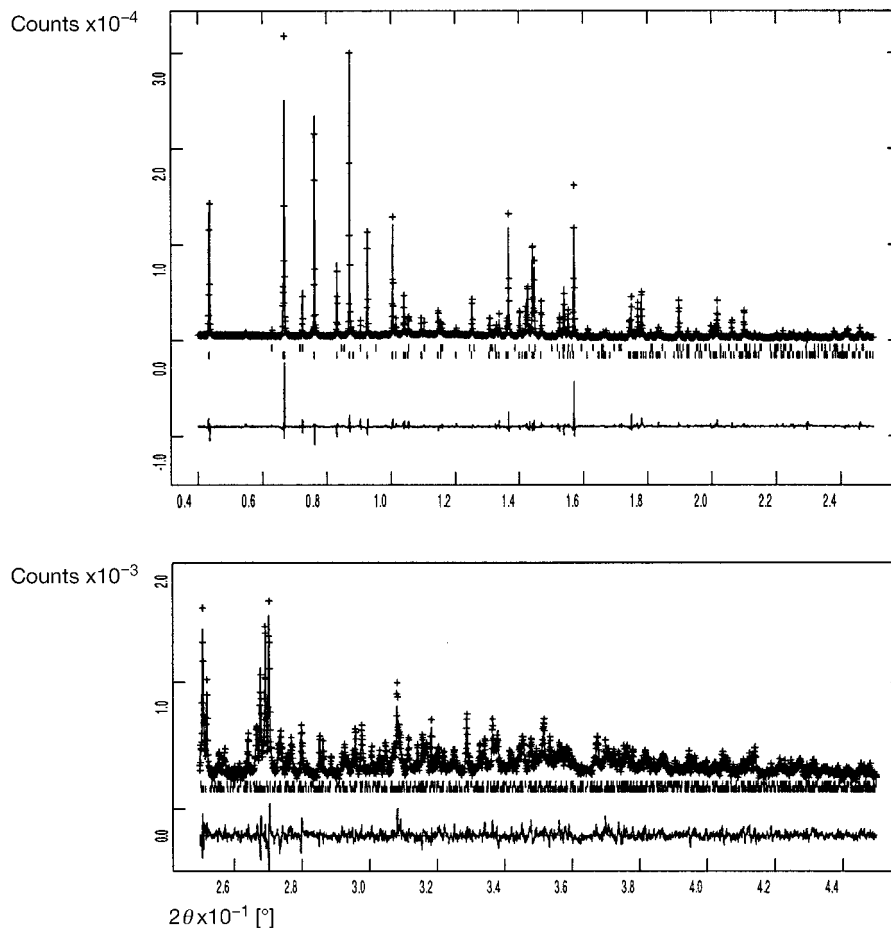


Fig. 2. Observed (+) and calculated (—) profiles for the Rietveld refinement for dihydrate **1** (above 5–25° and below 25–45°, different intensity scale). The bottom curve in each is the difference plot on the corresponding intensity scale.

involving the P–OH groups (O(6)–H $\cdots$ O(1W)<sup>e</sup>) and O(1)–H $\cdots$ O(2W)<sup>a</sup>); see Table 3). There are three H-bonds involving water molecules (O $\cdots$ O < 2.73 Å) in the coordination spheres of both P(1)O<sub>3</sub> and P(2)O<sub>3</sub> of **1**. Interestingly, the two strongest H-bonds (< 2.5 Å) of **1** involve water molecule O(W2), in contrast to compound **2** where the single water molecule participates in only one of the three strongest H-bonds. The H-atom positions, which were included in the refinement process to give a better agreement of the values of the calculated structural model and the measured data, have a relatively high error and, therefore a more detailed discussion of the distances and angles involved in H-bonding is not justified. The eight intermolecular H-bonds (O $\cdots$ O < 2.73 Å) involving one molecule of **1** and directed to neighbouring bis[phosphonic acid] molecules and water molecules, give rise to an extended three-dimensional network (Fig. 5).

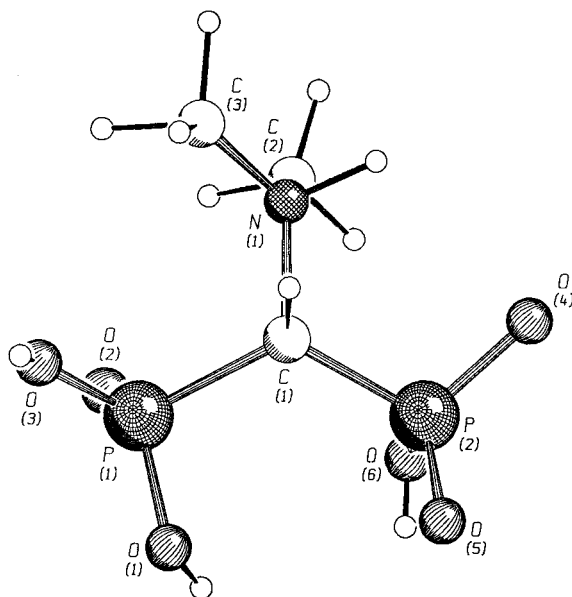


Fig. 3. Projection of the crystal structure of **1** perpendicular to the plane defined by the atoms P(1)–P(2)–N(1) showing the numbering scheme (SCHAKAL [16]). Arbitrary numbering.

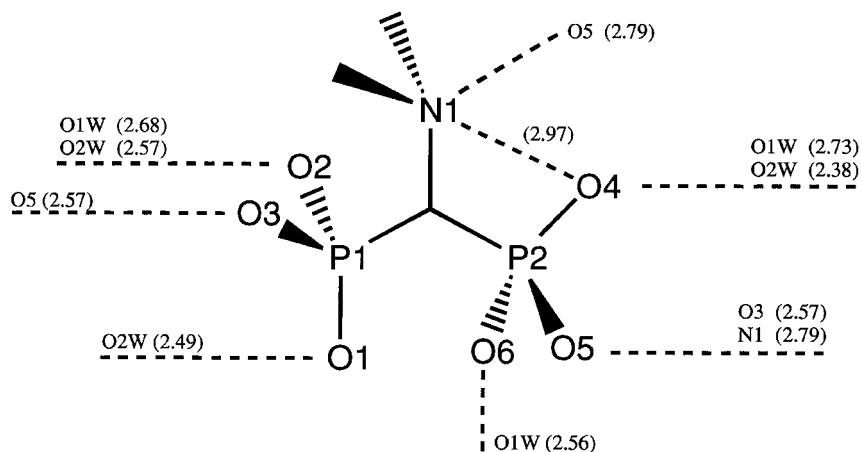


Fig. 4. The intra- and intermolecular contacts for compound **1** including the distances between non-H-atoms linked by H-bonds visualized by dashed lines

Since the two P-atoms in the molecule of **1** are nonequivalent, two signals arise in the solid-state  $^{31}\text{P}$ -NMR spectra. For all three compounds **1**–**3**, two lines are found, but the chemical shift of these two lines, while similar in the case of dihydrate **1** or monohydrate **2**, is very different in the case of the unhydrated form **3** (Table 4), *i.e.*, different solid-state NMR properties are observed. As there are no significant differences in the structure of the [(dimethylamino)methylene]bis[phosphonic acid]

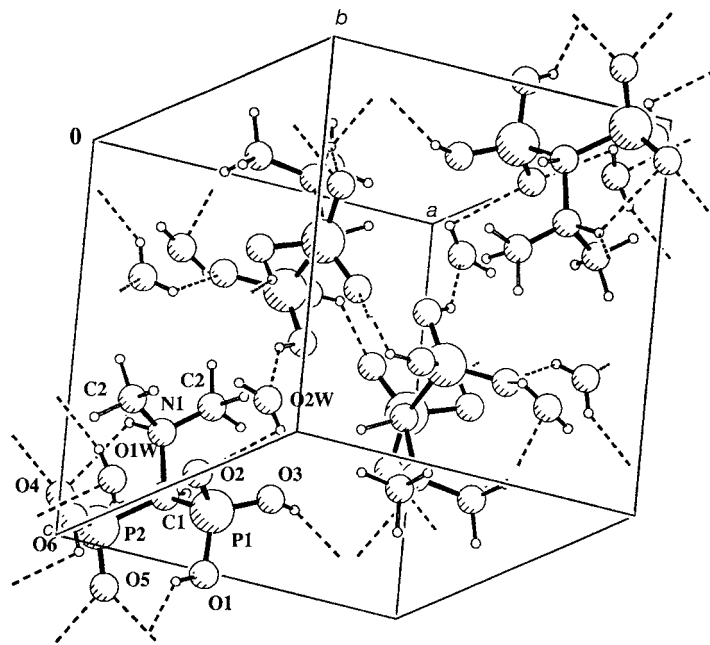


Fig. 5. A view of the structure of **1** down the *a* axis. The intermolecular contacts are shown by dashed lines (PLUTON [17]).

moiety of **1–3** (see Table 2), the reason for the different  $^{31}\text{P}$ -NMR chemical shifts must be due to the different environment of the two  $\text{PO}_3$  groups, specifically to their involvement in the intermolecular H-bonding network (Table 3). The environment of P(1) is similar in **1** and **2**. The bonding of the H-atoms to the atoms O(1) and O(3) is equivalent, and also the involvement of O(1), O(2), and O(3) in the H-bonding network is similar. The environment of P(2) of **1** and **2** differs only slightly, with the H-atom being connected to atom O(6) in the case of **1**, while in **2**, the H-atom is attached to atom O(4). Hence, the presence of water molecules in the coordination sphere of the  $\text{PO}_3$  groups results in a similar behaviour in the solid-state  $^{31}\text{P}$ -NMR of **1** and **2**.

Table 4. Solid-State  $^{31}\text{P}$ -NMR Data for **1–3**

	<b>1</b>	<b>2</b>	<b>3</b>
$\delta(\text{P})$ [ppm]	8.8, 7.0 [8]	8.4, 7.1 [18]	9.1, 2.0 [9] or 9.3, 2.3 [8]

The strongly differing chemical shifts of the two P-atoms of the unhydrated form **3** 9.1 and 2.0 ppm [9] or 9.3 and 2.3 ppm [8] are rationalized as follows. The atoms O(3) and O(6) of **3** are protonated, while a third proton is statistically distributed between atoms O(2) and O(5). Atoms O(1), O(2), and O(3) participate in the same H-bonds as atoms O(4), O(5), and O(6) (Table 3). The NH group of **1–3** participates in both an intra- and intermolecular H-bond. In all three compounds, the intramolecular contact involves the atom O(4). However, in **3**, the strong  $\text{N}(1)\text{--H}\cdots\text{O}$  intermolecular H-bond involves an O-atom connected to P(1), while in **1** and **2**, an O-atom connected to P(2) is



involved. These facts may explain the different solid-state  $^{31}\text{P}$ -NMR behaviour of **1** and **2** as compared to **3**.

This study shows that crystal structures can be solved by means of X-ray powder diffraction data and that the recording of high-resolution X-ray data can facilitate the study of two-phase problems. The powder structure analysis of dihydrate **1** established its overall three-dimensional structure, however, even though the high-resolution data permitted the free refinement of the non-H-atoms, the accuracy of this analysis is not comparable to that of the single-crystal structure analyses of **2** and **3**.

The authors would like to thank all group members of the Swiss-Norwegian Beam Line at ESRF, BP 220, F-38043 Grenoble Cédex, France, and of the Department of Chemistry of the Texas A & M University, Texas, USA, in particular the group of Prof. *Clearfield*, for enabling the diffraction experiments to be carried out. We also wish to thank the *Swiss National Science Foundation* for financial support and especially for a research grant for A. N.

## REFERENCES

- [1] C. F. Callis, A. F. Kerst, J. W. Lyons, 'Coordination Chemistry', Ed. S. Kirschner, Plenum Press, New York, 1969, p. 223.
- [2] M. D. Francis, R. G. G. Russell, L. H. Fleisch, *Science* **1969**, *165*, 1264.
- [3] U. Fischer, G. Hägele, *Z. Naturforsch., B* **1985**, *40*, 1152.
- [4] Y. Okaya, *Acta Crystallogr.* **1966**, *20*, 712.
- [5] H. Gross, B. Costisella, Th. Gnauk, L. Brennecke, *J. Prakt. Chem.* **1976**, *318*, 116.
- [6] S. Kulpe, I. Seidel, B. Costisella, *Z. Phys. Chem.* **1984**, *265*, 391.
- [7] L. M. Shkol'nikova, S. S. Sotman, E. G. Afonin, *Kristallografiya* **1990**, *35*, 1442.
- [8] H. Hancke, B. Costisella, K. Jancke, *Fresenius' J. Anal. Chem.* **1995**, *352*, 496.
- [9] R. K. Harris, L. H. Merwin, G. Hägele, *Magn. Reson. Chem.* **1989**, *27*, 470.
- [10] J. W. Visser, *J. Appl. Crystallogr.* **1969**, *2*, 89.
- [11] A. Altomare, M. C. Burla, G. Cascarano, C. Giacovazzo, A. Guagliardi, A. G. G. Moliterni, G. Polidori, 'EXPO, Program for Extracting Structure-Factor Amplitudes and Structure Solution from Powder Diffraction Data', Bari, Italy, 1997.
- [12] G. M. Sheldrick, *Acta Crystallogr., Sect. A* **1990**, *46*, 467.
- [13] G. M. Sheldrick, 'SHELXL-93, Program for Crystal Structure Refinement', University of Göttingen, Germany, 1993.
- [14] A. Larson, R. B. von Dreele, 'GSAS, Generalized Structure Analysis System', Los Alamos National Laboratory, Los Alamos, NM, 1994.
- [15] 'International Tables for Crystallography C', Kluwer Academic Publishers, Dordrecht, The Netherlands, 1995.
- [16] E. Keller, 'SCHAKAL, Program for the Graphic Representation of Molecular and Crystallographic Models, University of Freiburg, Germany, 1992.
- [17] A. L. Spek, *Acta Crystallogr., Sect. A* **1990**, *46*, C34.
- [18] L. H. Mervin, W. A. Dollase, G. Hägele, H. Blum, *Phosphorus, Sulfur, Silicon Relat. Elem.* **1991**, *50*, 117.

Received September 14, 1998